CHIN. PHYS. LETT. Vol. 38, No. 4 (2021) 043101

Configuration Interaction of Electronic Structure and Spectroscopy of AlH and Its Cation

Shu-Tao Zhao(赵书涛)[1,2*], Jun Li(李俊)[1], Rui Li(李瑞)[3*], Shuang Yin(阴爽)[3], and Hui-Jie Guo(国慧杰)[3]

[1]*School of Physics and Electronic Science, Fuyang Normal University, Fuyang 236037, China*
[2]*Institute of Atomic and Molecular Physics, Jilin University, Changchun 130012, China*
[3]*Department of Physics, College of Science, Qiqihar University, Qiqihar 161006, China*

(Received 20 December 2020; accepted 5 February 2021; published online 6 April 2021)

We carry out a detailed study of the low-lying states of AlH and AlH^+, using a multireference configuration interaction method. Based on the computed potential energy curves, the spectroscopic constants of bound Λ–S states are fitted; these agree with the results for the measurements. The values of the permanent dipole moment of the Λ–S states are calculated, and the charge transfer mechanism is discussed. Based on the calculated transition dipole moments and vibrational levels, the radiative lifetimes of bound states are determined. Finally, tunneling lifetimes, and $\nu' = 0$–2 vibrational levels of $4^2\Sigma^+$ and $3^2\Pi$ states with a potential barrier are investigated.

DOI: 10.1088/0256-307X/38/4/043101

Aluminum (Al), as the most abundant metal in the earth's crust (8%), is always found combined with hydrogen, oxygen, nitrogen, and light halides.[1–3] The aluminum hydride molecule (AlH) is the simplest hydride molecule containing Al, and its chemical[4–6] and astrophysical[7–9] significance have been an area of growing scientific interest for a long time, both theoretically and experimentally. As such, high-level calculation is required to further investigate the structures and transition properties of the complicated interaction of low-lying states in the AlH molecule and its cation.

Since the first spectrum observation of the AlH molecule in 1901 by Basquin,[10] many studies[11–13] of the electronic structures of the low-lying excited states and the ground state have been conducted. Furthermore, the radiative lifetimes of $A^1\Pi$ have been obtained using dye laser excitation.[14] The infrared spectra[15,16] have been observed by Fourier transform infrared emission spectroscopy, and the spectroscopic parameters[17] of the b–X and C–X transitions have been analyzed via ionization-detected spectra. In addition, the characteristics of the lower lying emission spectra of the AlH molecule have been identified.[18] Halfen and Ziurys[19,20] reported on the $J = 0 \rightarrow 1$ transition, examined using submillimeter direct absorption methods, and observed the A–X electronic transition. Szajna *et al.*[18] detected the high resolution A–X spectrum in the 22400–23700 cm^{-1} region, by means of dispersive optical spectroscopy.

Cade and Huo[21] have presented the potential energy curves (PECs) of second-row hydride (AlH, NaH, etc.) molecules via self-consistent field (SCF) calculations with Slater-type basis sets. Subsequently, the spectroscopic parameters and permanent dipole moments for the ground states of those diatomic hydride were calculated.[22] Soon afterwards, a number of theoretical calculations[23,24] for the PECs of AlH excited states were carried out. Barclay and Wright[25] described the effects of the frozen core approximation on the quality of their results, using different (He and Ne) cores, and compared these with values obtained in previous research. Woon and Dunning[26] have computed the electronic structures and spectroscopic parameters for the second-row diatomic hydride, using multireference configuration interaction (MRCI) calculations, and employing correlation-consistent basis sets of cc-pVXZ ($X = D, T, Q, 5$) quality to evaluate the spectroscopic constants of the ground state. They also estimated the complete basis set (CBS) limit, employing cc-pVXZ ($X = D, T, Q, 5$) basis sets. The convergence of the molecular properties, the structure, and the stability of AlH[27,28] have also been studied. Tao *et al.*[29] have reported their observations of the $b^3\Sigma^-$–$a^3\Pi$ band system of AlH and AlD, based on laser fluorescence excitation. Harata *et al.*[30] have studied the spectroscopic constants of the ground state, $X^1\Sigma^+$, of AlH, using coupled cluster (CCSD) methods. In re-

Supported by the National Natural Science Foundation of China (Grant No. 11604052), the Fundamental Research Funds in Heilongjiang Province Universities, China (Grant No.135109223), the Natural Science Research Project of the Education Department of Anhui Province, China (Grant No. KJ2020A0544), the Anhui Provincial Natural Science Foundation, China (Grant No. 1908085ME150), the Excellent Youth Talent Project of the Education Department of Anhui Province, China (Grant No. gxyqZD2019046), and the key Program of Excellent Youth Talent Project of Fuyang Normal University, China (Grant No. rcxm201801).
*Corresponding author. Email: zhaoshutao2002@163.com; ruili06@mails.jlu.edu.cn
© 2021 Chinese Physical Society and IOP Publishing Ltd

cent years, a wide variety of theoretical calculations relating to the AlH molecule have been acquired. Shi *et al.*[31] have investigated the electronic structure of AlH in terms of the multireference configuration interaction theory. A laser cooling scheme, using spin-allowed transitions of AlH and spin-forbidden transitions of AlF, has also been provided by Wells and Lane.[32]

With regard to AlH^+, only one $A^2\Pi$–$X^2\Sigma^+$ band system in the range of 27000–29000 cm^{-1} was detected by Szajna *et al.*, who utilized a traditional spectroscopic technique.[33] Their investigations demonstrate that the vibrational states of $A^2\Pi$ are perturbed by the nearby $B^2\Sigma^+$ state. Guest *et al.*[34] used the configuration interaction method to theoretically calculate the potential energy curves of the $^2\Sigma^+$ and $^2\Pi$ states. Nguyen *et al.*[35] investigated the electronic structures and transition properties of $X^2\Sigma^+$, $A^2\Pi$ and $B^2\Sigma^+$ at the MRCI level of theory. More recently, spectroscopic constants of AlH^+ have been obtained from the calculation of full-CI with a complete basis set, as performed by Ferrante *et al.*;[36] they considered core-correlation, relativistic, and diagonal Born–Oppenheimer contributions in their electronic structure calculations.

As stated above, a series of investigations have been conducted for low-lying states of AlH and AlH^+. However, only the electronic structures of low-lying excited states of AlH and AlH^+ have investigated before. An accurate assessment of the electronic structures of high excited states of AlH and AlH^+ remains to be performed, and the transition properties of high excited states have not been discussed before. In addition, the tunneling lifetimes of excited states with a potential barrier have not yet been investigated.

In this work, high-level configuration interaction calculations regarding the low-lying excited electronic states of AlH and AlH^+ are performed, using the MOLPRO program package,[37] and the spectroscopic parameters of bound states of AlH and AlH^+ are evaluated via the LEVEL[38] procedure. Single-point energy calculations are carried out for the C_{2v} group. A contracted Gaussian-type augmented correlation-consistent quintuple zeta all-electron aug-cc-pV5Z basis set[39,40] is selected for the H and Al atoms in our calculations. We study the Λ–S states of AlH and AlH^+ by means of the state-averaged complete active space self-consistent field (CASSCF) method.[41] In the CASSCF calculation, the active space is composed of $7a_1$, $3b_1$, $3b_2$ and $1a_2$ molecular orbitals (MOs). The 5 MOs ($3a_1$, $1b_1$, $1b_2$), correlating with $1s$, $2s$, and $2p$ shells of Al, are placed into a closed shell. In addition, we calculate the correlation energies of the excited states via the MRCI method.[42] The Davidson correction (+Q) is considered to reduce size-consistency error. Based on the calculated PECs, the spectroscopic constants of bound states are obtained from numerical solution of the nuclear Schrödinger equation. The radiative lifetimes of the low-lying vibrational levels of AlH and AlH^+ bound states are calculated using the calculated transition dipole moment (TDMs) and Franck–Condon factors (FCFs) in this work. The tunneling lifetimes of bound states with a potential barrier are obtained by the classical Wentzel–Kramers–Brillouin (WKB) method.[43]

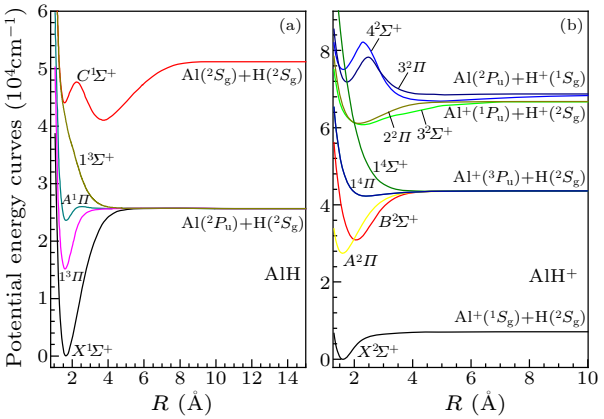

Fig. 1. Calculated PECs of the Λ–S states of AlH and its cation.

The PECs of the low-lying Λ–S states of AlH and AlH^+ have been studied here via the MRCI +Q method, as displayed in Figs. 1(a) and 1(b). Previous investigations have indicated the capacity of the configuration interaction method to exactly describe the dynamical correlation effect of electrons, and to provide accurate PECs for excited states.[44–47] As displayed in Fig. 1(a), the $C^1\Sigma^+$ state of AlH is associated with the second dissociation channel, Al(^2S_g)+H(^2S_g), and all of the other four states are correlated with the lowest dissociation channel, Al(^2P_u)+H(^2S_g). The energy gap between the second dissociation channel, Al(^2S_g)+H(^2S_g), and the first dissociation channel is 25533 cm^{-1}, which is in good agreement with the experimental result of 25348 cm^{-1}.[48] As shown in Fig. 1(b), the seven Λ–S states ($X^2\Sigma^+$, $A^2\Pi$, $B^2\Sigma^+$, $1^4\Pi$, $1^4\Sigma^+$, $2^2\Pi$ and $3^2\Sigma^+$) associate with three lowest dissociation limits, Al$^+$(^1S_g)+H(^2S_g), Al$^+$(^3P_u)+H(^2S_g), and Al$^+$(^1P_u)+H(^2S_g), and the other states, $4^2\Sigma^+$ and $3^2\Pi$, associate with the fourth dissociation limit, [Al(^2P_u)+H$^+$(^1S_g)], which indicates charge-transfer from Al to H. The energy gaps between the fourth, third, and second dissociation channels with respect to the lowest dissociation channel are 36464 cm^{-1}, 59631 cm^{-1}, and 61152 cm^{-1}, which closely resemble the experimental results of 37392 cm^{-1}, 59854 cm^{-1}, and 61411 cm^{-1}.[48]

The spectroscopic constants of the AlH and AlH^+ bound states are evaluated and listed in Table 1, where the previous experimental and theoretical spectroscopic constants are also given. For the ground

state, $X^1\Sigma^+$, of AlH, the dominant electronic configuration is $4\sigma^2 5\sigma^2$, and our calculated spectroscopic constants at the MRCI +Q level are closed to the previously observed values,[49] with deviations of 0.006 Å, 8 cm^{-1}, 2 cm^{-1}, and 0.04 cm^{-1} for R_e, ω_e, $\omega_e x_e$, and B_e, respectively. The electronic configurations of the second excited state, $1^3\Pi$, and the third excited state, $A^1\Pi$, are formed by $5\sigma \rightarrow 2\pi$ one-electron promotion. There has been little research relating to the $1^3\Pi$ state in previous studies. The $1^3\Pi$ state sits between the ground state, $X^1\Sigma^+$, and the $A^1\Pi$ state. The PEC of the $A^1\Pi$ state has a small barrier at $R \sim 2.5$ Å, owing to the interaction of the attractive and repulsive valence state configurations. Here, R_e and ω_e are computed to be 1.665 Å and 1370 cm^{-1}, closely in agreement with the experimental results[18] of 1.65 Å and 1416 cm^{-1}. The PEC of $C^1\Sigma^+$ state exhibits double-well characteristics, in line with previous theoretical investigations[50] and experimental results.[18,51] The dominant electronic configurations of the inner and outer wells of $C^1\Sigma^+$ are $4\sigma^2 5\sigma^1 6\sigma^1$ (92.2%) and $4\sigma^2 5\sigma^2$ (46.6%), $4\sigma^2 5\sigma^1 6\sigma^1$ (14.5%), and $4\sigma^2 5\sigma^1 7\sigma^1$ (11.6%). The outer well of $C^1\Sigma^+$ exhibits a mixture of three electronic configurations, confirming that a multireference configuration interaction method should be applied in the calculation. The spectroscopic parameters of the two potential wells are provided in Table 1.

Table 1. Computed spectroscopic constants of the Λ–S states of AlH.

Λ–S state	T_e (cm^{-1})	R_e (Å)	ω_e (cm^{-1})	$\omega_e x_e$ (cm^{-1})	B_e (cm^{-1})	Electronic configuration at R_e	References
AlH							
$X^1\Sigma^+$	0	1.654	1675	27	6.35	$4\sigma^2 5\sigma^2$ (89.8%)	This work
	0		1682	29	6.39		Expt.[52]
	0	1.648	1683	29	6.39		Expt.[49]
	0	1.647	1741	27	6.39		Calc.[21]
	0	1.678	1663	30	6.16		Calc.[23]
	0	1.644	1704	29	6.42		Calc.[22]
	0	1.652	1679	29	6.360		Calc.[50]
	0	1.653	1686				Calc.[9]
	0	1.652	1728	27	6.362		Calc.[25]
	0	1.653	1680	29	6.35		Calc.[26]
	0	1.672					Calc.[27]
	0	1.640	1690		6.45		Calc.[28]
	0	1.649	1690	30	6.378		Calc.[30]
	0	1.651	1683	29	6.366		Calc.[31]
$1^3\Pi$	15115	1.600	2012	94	6.79	$4\sigma^2 5\sigma^1 2\pi^1$ (93.4%)	This work
$A^1\Pi$	23536	1.665	1370	125	6.34	$4\sigma^2 5\sigma^1 2\pi^1$(87.3%)	This work
		1.65	1416	166	6.39		Expt.[18]
		1.648			6.39		Expt.[49]
		1.673			6.39		Calc.[50]
$C^1\Sigma^+$ (inner well)	43999	1.575	1566	100	7.15	$4\sigma^2 5\sigma^1 6\sigma^1$(92.2%)	This work
		1.61	1575	126	6.67		Expt.[18]
	44675	1.613	1575	126	6.67		Expt.[51]
	44519	1.621					Calc.[50]
$C^1\Sigma^+$ (outer well)	41049	3.735	491	6	1.24	$4\sigma^2 5\sigma^2$ (46.6%) $4\sigma^2 5\sigma^1 6\sigma^1$ (14.5%) $4\sigma^2 5\sigma^1 7\sigma^1$ (11.6%)	This work
	40892	3.76	478	6	12.31		Calc.[50]
AlH^+							
$X^2\Sigma^+$	0	1.606	1651	96	6.76	$4\sigma^2 5\sigma^1$ (92.2%)	This work
	0	1.6018	1620		6.763		Expt.[49]
	0	1.6098	1684.4	80.78	6.698		Calc.[34]
$A^2\Pi$	27434	1.599	1840	47	6.81	$4\sigma^2 2\pi^1$ (86.2%) $4\sigma^1 5\sigma^1 2\pi^1$(5.9%)	This work
	27593	1.5914	1770		6.851		Expt.[49]
		1.6047	1727.0	54.37	6.741		Calc.[34]
$B^2\Sigma^+$	30862	2.058	1388	32	4.10	$4\sigma^1 5\sigma^2$ (74.4%) $4\sigma^2 6\sigma^1$ (14.6%) $4\sigma^1 2\pi^2$ (4.2%)	This work
		2.0582	1321.5	19.48	4.097		Calc.[34]
$3^2\Sigma^+$	60721	2.294	582	16	3.30	$4\sigma^2 6\sigma^1$ (71.3%) $4\sigma^1 5\sigma^2$ (14.5%) $4\sigma^1 5\sigma^2$ (1.9%)	This work
		2.3655	624.6	11.55	3.102		Calc.[34]
$2^2\Pi$	61100	2.131	718	17	3.78	$4\sigma^1 5\sigma^1 2\pi^1$ (67.8%) $4\sigma^2 3\pi^1$ (18.6%)	This work
		2.2033	701.3	36.026	3.576		Calc.[34]
$3^2\Pi$	71824	1.745	1728	67	5.70	$4\sigma^1 5\sigma^1 2\pi^1$ (68.1%) $4\sigma^2 3\pi^1$ (14.5%)	This work
$4^2\Sigma^+$	75019	1.613	1791	47	6.68	$4\sigma^2 8\sigma^1$(89.8%)	This work
$1^4\Pi$	42285	2.433	436	37	2.94	$4\sigma^1 5\sigma^1 2\pi^1$ (97.8%)	This work

The equilibrium internuclear distance of the inner and outer wells are 1.575 Å and 3.735 Å, respectively, and the calculated spectroscopic constants excellently reproduce the previous results of 1.621 Å and 3.76 Å.[50] The deviations of the inner well are only 676 cm^{-1}, 0.035 Å, 9 cm^{-1}, 26 cm^{-1}, and 0.48 cm^{-1} for T_e, R_e, ω_e, $\omega_e x_e$ and B_e, respectively.[18,51] As for the outer well, our calculated values of T_e, R_e, and ω_e differ by 157 cm^{-1}, 0.025 Å, and 13 cm^{-1}, respectively, from the previous theoretical results.[50]

For the $X^2\Sigma^+$of AlH^+, the electronic configuration can primarily be described by $4\sigma^2 5\sigma^1$ (92.2%). Our MRCI calculated R_e, ω_e, and B_e, for $X^2\Sigma^+$, are 1.606 Å, 1651 cm^{-1}, and 6.76 cm^{-1}, respectively, which is in good agreement with the corresponding experimental results of 1.6018 Å, 1620 cm^{-1}, and 6.763 cm^{-1}.[49] As for the first excited state, $A^2\Pi$, the electronic configuration arises from $5\sigma \rightarrow 2\pi$ one-electron excitation, and $4\sigma \rightarrow 2\pi$ one-electron excitation. Our calculated spectroscopic constants closely resemble the experimental results,[49] and deviations are only 159 cm^{-1}, 0.008 Å, 70 cm^{-1}, and 0.04 cm^{-1} for T_e, R_e, ω_e, and B_e. Overall, our calculated spectroscopic constants fit very well with the previous experimental results.

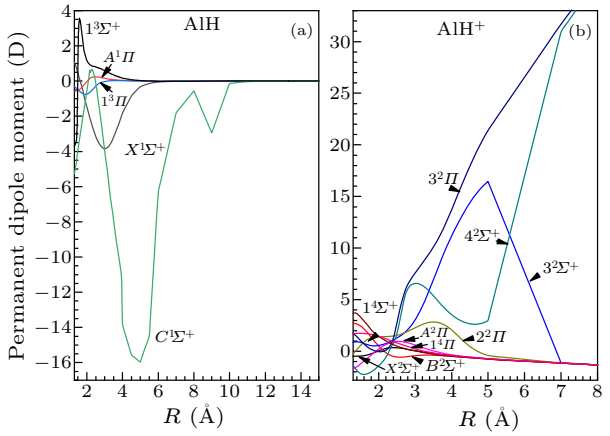

Fig. 2. Permanent dipole moments of the Λ–S states as a function of internuclear distance R.

The permanent dipole moment curves of AlH and AlH^+ are plotted in Figs. 2(a) and 2(b). As shown in Fig. 2(a), at the internuclear distance, R_e, the permanent dipole moment of $X^1\Sigma^+$ is computed to be 0.094 Debye(D) with a Al^+H^- polarity. The permanent dipole moment curves of $X^1\Sigma^+$, $A^1\Pi$, $1^3\Sigma^+$,$1^3\Pi$, and $C^1\Sigma^+$ are all close to zero at the large internuclear distance R = 15.00 Å, indicating the neutral product of the first and second dissociation channels. At R = 4.85 Å, the permanent dipole moment of $C^1\Sigma^+$ exhibits a large value, reflecting the obvious ionic characterization of the $C^1\Sigma^+$ state. As displayed in Fig. 2(b), at the internuclear distance R_e, the dipole moment of $X^2\Pi$ is −0.038 D. When the internuclear distance increases to R = 8.00 Å, the permanent dipole moments of $3^2\Pi$ and $4^2\Sigma^+$ in the fourth dissociation limit, $Al(^2P_u)+H^+(^1S_g)$, approach large positive values, while the permanent dipole moments of other states of the three lowest dissociation limits tend to small negative values. At the large internuclear distance of R = 8.0 Å, the change of sign in permanent dipole moments of the fourth dissociation limit, with respect to the three lowest dissociation limits, reflects the phenomenon of charge transfer.

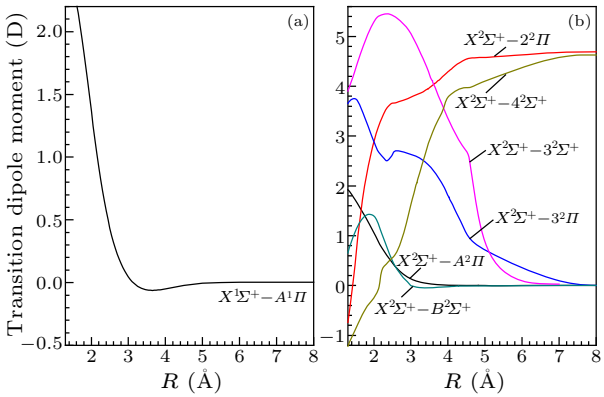

Fig. 3. Transition dipole moments of AlH and AlH^+.

Based on the MRCI calculations, we obtain the transition dipole moments (TDMs) of AlH and AlH^+, as shown in Figs. 3(a) and 3(b). At an equilibrium distance of R = 1.654 Å, the TDM of the $X^1\Sigma^+$–$A^1\Pi$ states of AlH exhibits a large value of 2.140 D. The TDMs of $X^1\Sigma^+$–$A^1\Pi$ decrease gradually with increasing internuclear distance, and the TDM of $X^1\Sigma^+$–$A^1\Pi$ approaches a minimum value at R = 3.630 Å. At the distance of R = 1.606 Å, the TDMs of $X^2\Sigma^+$–$A^2\Pi$ and $X^2\Sigma^+$-$B^2\Sigma^+$ states of AlH^+ are calculated to be 1.600 D and 1.300 D, respectively. The TDMs from other excited states of AlH^+ to the $X^2\Sigma^+$ state also exhibit non-negligible values in the Franck–Condon region. On the basis of calculated vibrational levels and TDMs, the radiative lifetimes of vibrational levels of AlH and AlH^+ bound states are evaluated via the formula

$$\begin{aligned}\tau\nu' &= (A\nu')^{-1} \\ &= \frac{3\mathrm{h}}{64\pi^4|a_0 \times e \times \mathrm{TDM}|^2 \Sigma_{v''} q_{v'v''}(E^3_{v'v''})} \\ &= \frac{4.9355 \times 10^5}{|\mathrm{TDM}|^2 \Sigma_{v'} q_{v'v''}(E^3_{v'v''})}, \end{aligned} \quad (1)$$

where $q_{\nu'\nu''}$ is the Franck–Condon factor (FCF), TDM is the transition dipole moment at the equilibrium distance, and $E_{\nu'\nu''}$ is the energy gap between the ν'–ν'' states. The lifetimes of the low-lying vibrational levels of AlH and AlH^+ bound states are provided in Table 2. Our calculated radiative lifetimes for the $\nu' = 0$ and $\nu' = 1$ vibrational levels of the $A^1\Pi$ state of AlH are 61.1 ns and 80.9 ns, respectively, and agree well with the experimental measurements of 66 ns and 83 ns.[14]

The radiative lifetime for the $\nu' = 0$ vibrational level of the $A^2\Pi$ state of AlH^+ is calculated to be 63.0 ns, which agrees well with a previous theoretical result of 61 ns.[35] In this work, we also calculate the radiative lifetimes of the $B^2\Sigma^+$, $3^2\Sigma^+$, $2^2\Pi$, $4^2\Sigma^+$, and $3^2\Pi$ states of AlH^+. The radiative lifetimes of the $\nu' = 0$ vibrational levels of $B^2\Sigma^+$ and $3^2\Pi$ are on the order of 10 ns, while the radiative lifetimes of $\nu' = 0$ vibrational levels of $3^2\Sigma^+$, $2^2\Pi$, and $4^2\Sigma^+$ are on the order of 1 ns. Since the PECs of $4^2\Sigma^+$ and $3^2\Pi$ both have a potential barrier above the fourth dissociation limit, $Al(^2P_u)+H^+(^1S_g)$, the vibrational states of the $4^2\Sigma^+$ and $3^2\Pi$ states can decay into the continuum by means of barrier penetration. Utilizing the WKB method, the tunneling lifetimes of the three lowest vibrational levels of the $4^2\Sigma^+$ and $3^2\Pi$ states are calculated and listed in Table 2. The natural lifetime of a given vibrational state can be expressed by the formula

$$\frac{1}{\tau_{\text{natural}}} = \frac{1}{\tau_{\text{radiative}}} + \frac{1}{\tau_{\text{tunneling}}}, \tag{2}$$

where $\tau_{\text{radiative}}$ and $\tau_{\text{tunneling}}$ are the radiative lifetime and tunneling lifetime of the vibrational state. The $\tau_{\text{tunneling}}$ values of the $\nu' = 0$ and $\nu' = 1$ vibrational states of the $4^2\Sigma^+$ and $3^2\Pi$ states are at least two orders of magnitude larger than the corresponding radiative lifetimes. Hence, the natural lifetimes of $\nu' = 0$ and $\nu' = 1$ vibrational states of $4^2\Sigma^+$ and $3^2\Pi$ are shown to originate mainly from radiative lifetimes. For the $\nu' = 2$ vibrational state of $4^2\Sigma^+$ and $3^2\Pi$, the tunneling lifetimes are smaller than the corresponding radiative lifetimes, so the natural lifetimes of the $\nu' = 2$ vibrational state for the two states primarily originate from tunneling lifetimes.

Table 2. Lifetimes (ns) of low-lying states of AlH and AlH^+.

State	ν'	Radiative lifetimes (ns)	Tunneling lifetimes (ns)	Natural lifetimes (ns)
$A^1\Pi$	0	61.1		61.1
	1	80.9		80.9
$A^2\Pi$	0	63.0		63.0
	1	68.7		68.7
$B^2\Sigma^+$	0	90.6		90.6
	1	97.3		97.3
	2	113.7		113.7
$3^2\Sigma^+$	0	0.6		0.6
	1	0.6		0.6
	2	0.7		0.7
$2^2\Pi$	0	1.6		1.6
	1	1.6		1.6
	2	1.7		1.7
$4^2\Sigma^+$	0	0.8	0.2×10^8	0.8
	1	1.3	3.1×10^3	1.3
	2	2.7	1.6	1.0
$3^2\Pi$	0	20.0	1.4×10^8	20.0
	1	82.5	5.8×10^3	81.3
	2	121.5	2.2	2.2

In summary, we have computed the PECs and permanent dipole moment curves of the Λ–S states of AlH and AlH^+ at the MRCI level. Based on the calculated PECs, the accurate spectroscopic parameters of AlH and AlH^+ bound states have been obtained, and are in accordance with the experimental results. The TDMs of spin-allowed transitions of AlH and AlH^+ have also been calculated. Based on the calculated TDMs and vibrational levels, the radiative lifetimes of low-lying vibrational levels of AlH and AlH^+ are evaluated, and agree well with the existing experimental results. Utilizing the WKB method, the tunneling lifetimes of $\nu' = 0$–2 vibrational levels for the $4^2\Sigma^+$ and $3^2\Pi$ states have been determined, and the competitive mechanism between tunneling lifetimes and radiative lifetimes for $4^2\Sigma^+$ and $3^2\Pi$ are discussed. It is anticipated that this work will lead to an improved understanding of the spectroscopic properties of excited states of AlH and AlH^+.

Acknowledgments.—The authors wish to express their thanks to Professor Bing Yan, in Institute of Atomic and Molecular Physics, Jilin University, for useful discussion.

References

[1] Tzeli D and Mavridis A 2001 *J. Phys. Chem. A* **105** 1175
[2] Leskiw B D, Castleman A W, Ashman C and Khanna S N 2001 *J. Chem. Phys.* **114** 1165
[3] Allendorf M D, Melius C F, Cosic B and Fontijn A 2002 *J. Phys. Chem. A* **106** 2629
[4] Zhang Y and Stuke M 1988 *J. Cryst. Growth* **93** 143
[5] Erlandson A C and Cool T A 1984 *J. Appl. Phys.* **56** 1325

[6] Ram R S and Bernath P F 1996 *Appl. Opt.* **35** 2879
[7] Sotirovski P 1972 *Astron. Astrophys. Suppl. Ser.* **6** 85
[8] Johnson H and Sauval A 1982 *Astron. Astrophys. Suppl. Ser.* **49** 77
[9] Bauschlicher C W and Langhoff S R 1988 *J. Chem. Phys.* **89** 2116
[10] Basquin O H 1901 *Astrophys. J.* **14** 1
[11] Zeeman P B and Ritter G J 1954 *Can. J. Phys.* **32** 555
[12] Deutsch J L, Neil W S and Ramsay D A 1987 *J. Mol. Spectrosc.* **125** 115
[13] Holst W and Hulthén E 1934 *Z. Phys.* **90** 712
[14] Baltayan P and Nedelec O 1979 *J. Chem. Phys.* **70** 2399
[15] White J B, Dulick M and Bernath P F 1993 *J. Chem. Phys.* **99** 8371
[16] Urban R D and Jones H 1992 *Chem. Phys. Lett.* **190** 609
[17] Zhu Y F, Shehadeh R and Grant E R 1992 *J. Chem. Phys.* **97** 883
[18] Szajna W, Zachwieja M, Hakalla R *et al.* 2011 *Acta Phys. Pol. A* **120** 417
[19] Halfen D T and Ziurys L M 2004 *Astrophys. J.* **607** L63
[20] Halfen D T, Ziurys L M 2010 *Astrophys. J.* **713** 520
[21] Cade P and Huo W 1967 *J. Chem. Phys.* **47** 649
[22] Meyer W and Rosmus P 1975 *J. Chem. Phys.* **63** 2356
[23] Pelissier M and Malrieu J P 1977 *J. Chem. Phys.* **67** 5963
[24] Sabelli N H, Kantor M, Benedek R and Gilbert T L 1978 *J. Chem. Phys.* **68** 2767
[25] Barclay V J and Wright J S 1988 *Chem. Phys.* **121** 381
[26] Woon D E and Dunning T H 1993 *J. Chem. Phys.* **99** 1914
[27] Schwerdtfeger P and Ischtwan J 1994 *J. Mol. Struct.: THEOCHEM* **306** 9
[28] Gutsev G L, Jena P and Bartlett R J 1999 *J. Chem. Phys.* **110** 2928
[29] Tao C, Tan X, Dagdigian P J and Alexander M H 2003 *J. Chem. Phys.* **118** 10477
[30] Hirata S, Yanai T, de Jong W A, Nakajima T and Hirao K 2004 *J. Chem. Phys.* **120** 3297
[31] Shi D H, Liu H, Zhang X N, Sun J F, Liu Y F and Zhu Z L 2011 *Int. J. Quantum Chem.* **111** 554
[32] Wells N and Lane I C 2011 *Phys. Chem. Chem. Phys.* **13** 19018
[33] Szajna W and Zachwieja M 2011 *J. Mol. Spectrosc.* **269** 56
[34] Guest M F and Hirst D M 1981 *Chem. Phys. Lett.* **84** 167
[35] Nguyen J H V, Viteri C R, Hohenstein E G, Sherrill C D, Brown K R and Odom B 2011 *New J. Phys.* **13** 063023
[36] Ferrante F, Prestianni A and Armata N 2017 *Theor. Chem. Acc.* **136** 3
[37] Werner H J, Knowles P J, Knizia G, Manby F R, Schütz M 2012 *Molpro: A General-purpose Quantum Chemistry Program Package* in *WIREs Computational Molecular Science* **2** 242
[38] Le R R J 2017 *J. Quant. Spectrosc. Radiat. Transfer* **186** 167
[39] Woon D E and Dunning T H 1993 *J. Chem. Phys.* **98** 1358
[40] Dunning T H 1989 *J. Chem. Phys.* **90** 1007
[41] Knowles P J and Werner H J 1985 *Chem. Phys. Lett.* **115** 259
[42] Werner H J and Knowles P J 1988 *J. Chem. Phys.* **89** 5803
[43] Ford K W, Hill D L, Wakano M and Wheeler J A 1959 *Ann. Phys.* **7** 239
[44] Wang K, Wang X X, Qu Y Z, Liu C H, Liu L, Wu Y and Buenker R J 2020 *Chin. Phys. Lett.* **37** 023401
[45] Liang G Y, Peng Y G, Li R, Wu Y and Wang J G 2020 *Chin. Phys. Lett.* **37** 123101
[46] Zhang X, Liu J P, Li J G and Zou H X 2019 *Chin. Phys. Lett.* **36** 113101
[47] Zhang D H, Xie L Y, Jiang J and Dong C Z 2019 *Chin. Phys. Lett.* **36** 083401
[48] Moore C E 1971 *Atomic Energy Levels* (Washington, DC: National Bureau of Standard)
[49] Huber K P and Herzberg G 1979 *Molecular Spectra and Molecular Structure: IV Constants of Diatomic Molecules* (New York: Van Nostrand Reinhold)
[50] Mauricio J, Matos O, Malmqvist P and Roos B O 1987 *J. Chem. Phys.* **86** 5032
[51] Szajna W and Zachwieja M 2010 *J. Mol. Spectrosc.* **260** 130
[52] Szajna W and Zachwieja M 2009 *Eur. Phys. J. D* **55** 549